Next-to-next-to-leading-order QCD corrections to pion electromagnetic form factors

Based on arXiv: 2403.04762

Wen Chen

South China Normal University

in collaboration with Long-bin Chen (GZHU), Feng Feng (CUMTB), Yu Jia (IHEP)

Apr. 07, 2024
@ HUST (Wuhan)

Contents

Introduction

Introduction

Electromagnetic form factor

$$\langle \pi^+(P')|J^\mu_{\rm em}|\pi^+(P)\rangle = F_\pi(Q^2)(P^\mu + P'^\mu)\,. \tag{1}$$

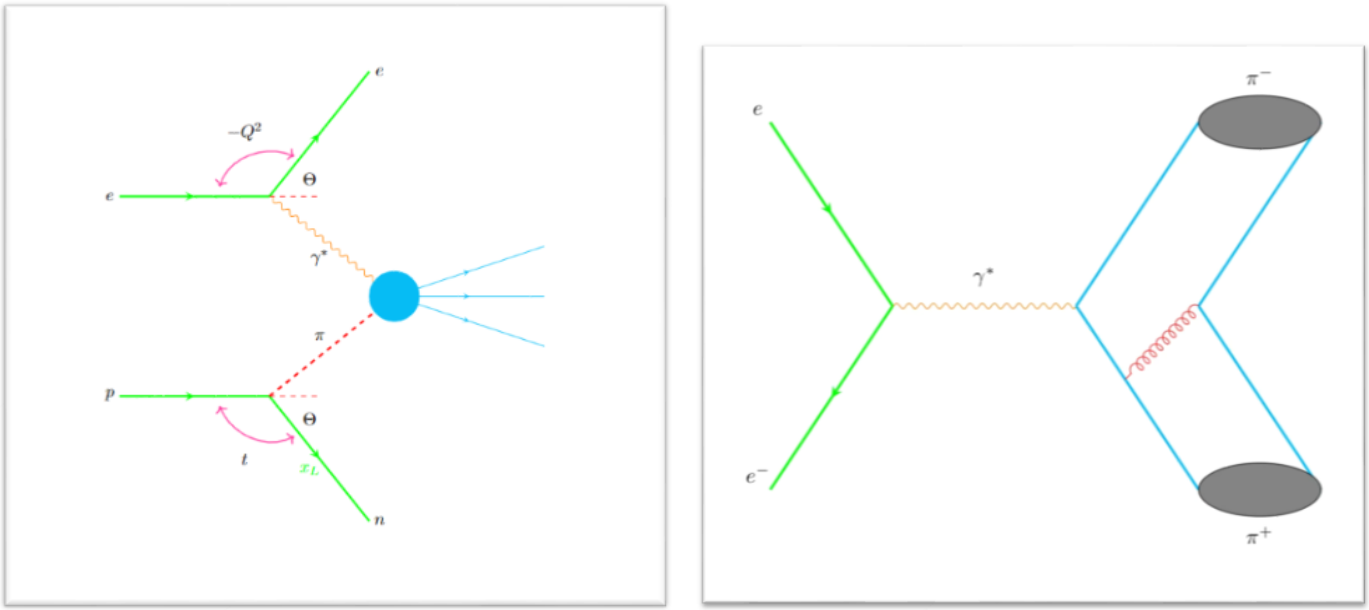

Figure: Measurements of the pion form factor.

For the lattice-QCD calculations, see Ding's talk.

Collinear factorization

hard scattering kernel (perturbative)

$$F_\pi(Q^2) = \iint dx\, dy\, \Phi^*_\pi(x,\mu_F) T(x,y,\frac{\mu_R^2}{Q^2},\frac{\mu_F^2}{Q^2}) \Phi_\pi(y,\mu_F)\,. \tag{2}$$

Light-cone distribution amplitude (LCDA)

Wilson line

$$\Phi_\pi(x,\mu_F) = \int \frac{dz^-}{2\pi i} e^{iz^- xP^+} \left\langle 0 \left| \bar{d}(0)\gamma^+\gamma_5 \mathcal{W}(0,z^-) u(z^-) \right| \pi^+(P) \right\rangle\,. \tag{3}$$

Efremov-Radyushkin- Brodsky-Lepage (ERBL) evolution equation

$$\frac{d\Phi_\pi(x,\mu_F)}{d\ln\mu_F^2} = \int_0^1 dy\, V(x,y)\, \Phi_\pi(y,\mu_F)\,. \tag{4}$$

We focus on the next-to-next-to-leading order calculation of the hard-scattering kernel.

History

- Leading order
  Chernyak et al.(1977)JETPL, Farrar&Jackson(1979)PRL, Chernyak&Zhitnitsky(1980)SJNP, Lepage&Brodsky(1979)PRL, (1980)PRD, Efremov&Radyushkin(1980)PLB, Duncan&Mueller(1980)PRD
- Next-to-leading order
  Field et al.(1981)NPB, Dittes&Radyushkin(1981)SJNP, Sarmadi(1984)PLB, Braaten&Tse(1987)PRD, Melic et al.(1999)PRD

photon-pion form factor
Gao et al. (2022) PRL, Braun et al. (2021) PRD

Calculation of hard-scattering kernel

Calculation of hard-scattering kernel

The hard-scattering kernel is insensitive to the long-distance physics.

$$\Phi_{\pi,\text{bare}} \to \delta(x-u)\,. \tag{5}$$

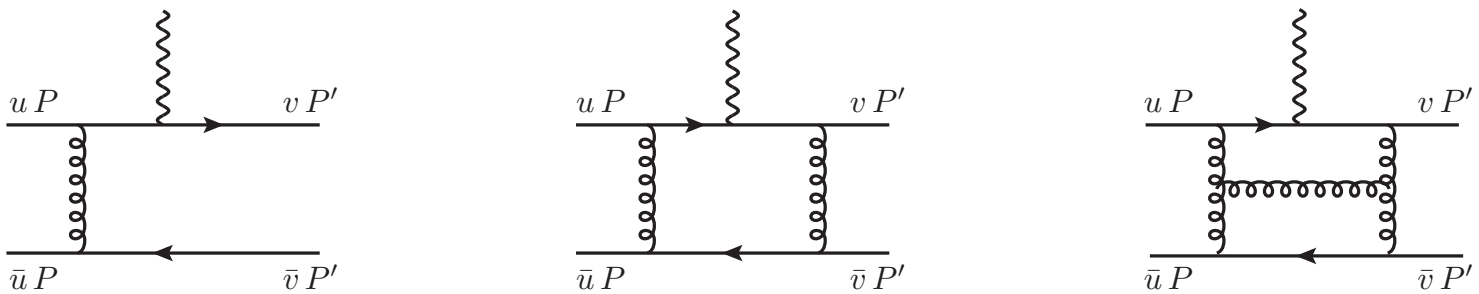

Figure: Sample parton-level Feynman diagrams for the reaction $\gamma^*\pi(P) \to \pi(P')$ at various perturbative orders.

Modern techniques on Feynman amplitude calculations

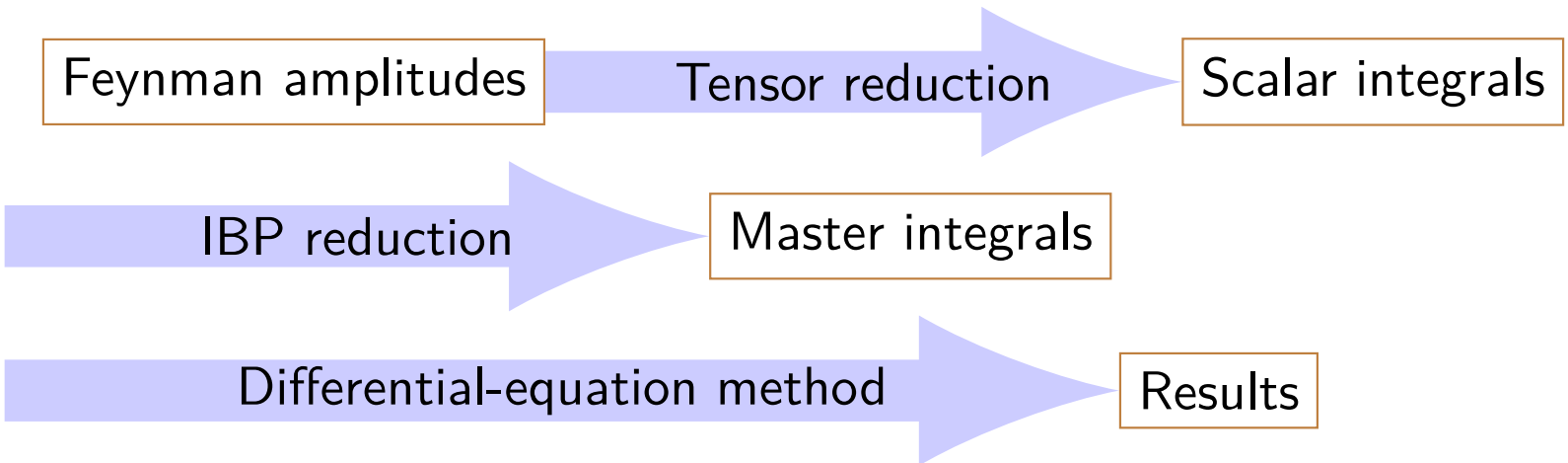

Differential-equation method

$$\frac{\partial}{\partial y} I_i = \sum_j M_{ij} I_j \,. \tag{6}$$

master integrals

Boundary conditions

$$I_i = \sum_a y^{\lambda_a} I_{i,a} \,. \tag{7}$$

The boundary integrals $I_{i,a}$ can be reduced in the parametric representation Chen (2020) JHEP, (2020) EPJC, (2021) EPJC

Single-scale boundary integrals can be calculated recursively in the parametric representation. Chen, Luo, Yang, Zhu (2024) JHEP

Renormalization

$$\Phi(x|u) = \int dy Z(x,y)\Phi_{\rm bare}(y|u) = Z(x,u)\,. \tag{8}$$

$$Z(x,y) = \delta(x-y) + \sum_{k=1}^{\infty} \frac{1}{\epsilon^k} Z_k(x,y)\,. \tag{9}$$

$$\alpha_s \frac{\partial Z_{n+1}}{\partial \alpha_s} = \alpha_s \frac{\partial Z_1}{\partial \alpha_s} \otimes Z_n + \beta(\alpha_s)\frac{\partial Z_n}{\partial \alpha_s}\,. \tag{10}$$

$$V(x,y) = -\alpha_s \partial Z_1/\partial \alpha_s\,. \tag{11}$$

Perturbative matching

$$F(u,v) = F^{(0)}(u,v) + \frac{\alpha_s}{\pi} F^{(1)}(u,v) + \left(\frac{\alpha_s}{\pi}\right)^2 F^{(2)}(u,v) + \cdots ; \tag{12}$$

$$T = T^{(0)} + \frac{\alpha_s}{\pi} T^{(1)} + \left(\frac{\alpha_s}{\pi}\right)^2 T^{(2)} + \cdots ; \tag{13}$$

$$\Phi(x|u) = \Phi^{(0)}(x|u) + \frac{\alpha_s}{\pi} \Phi^{(1)}(x|u) + \left(\frac{\alpha_s}{\pi}\right)^2 \Phi^{(2)}(x|u) + \cdots . \tag{14}$$

$$Q^2 F^{(0)}(u,v) = T^{(0)}(u,v) ; \tag{15}$$

$$Q^2 F^{(1)}(u,v) = T^{(1)}(u,v) + \Phi^{(1)}(x|u) \underset{x}{\otimes} T^{(0)}(x,v) + \Phi^{(1)}(y|v) \underset{y}{\otimes} T^{(0)}(u,y) ; \tag{16}$$

$$\begin{aligned} Q^2 F^{(2)}(u,v) = {} & T^{(2)}(u,v) + \Phi^{(2)}(x|u) \underset{x}{\otimes} T^{(0)}(x,v) + \Phi^{(2)}(y|v) \underset{y}{\otimes} T^{(0)}(u,y) \\ & + \Phi^{(1)}(x|u) \underset{x}{\otimes} T^{(1)}(x,v) + \Phi^{(1)}(y|v) \underset{y}{\otimes} T^{(1)}(u,y) \\ & + \Phi^{(1)}(x|u) \underset{x}{\otimes} T^{(0)}(x,y) \underset{y}{\otimes} \Phi^{(1)}(y|v) . \end{aligned} \tag{17}$$

$$\Phi_\pi(x,\mu_F) = \frac{f_\pi}{2\sqrt{2N_c}} \sum_{n=0}{}' a_n(\mu_F)\psi_n(x), \tag{18}$$

$$\psi_n(x) = 6x\bar{x}C_n^{3/2}(2x-1). \tag{19}$$

Gegenbauer polynomial

$$Q^2 F_\pi(Q^2) = \frac{2C_F\pi^2(e_u-e_d)f_\pi^2}{3} \sum_{k=0} \left(\frac{\alpha_s}{\pi}\right)^{k+1} \sum_{m,n}{}' a_n(\mu_F)a_m(\mu_F)\mathcal{T}_{mn}^{(k)}, \tag{20}$$

$$\mathcal{T}_{mn}^{(k)} = \frac{1}{e_u-e_d}\psi_m(x) \underset{x}{\otimes} T^{(k)}\left(x,y,\frac{\mu_R^2}{Q^2},\frac{\mu_F^2}{Q^2}\right) \underset{y}{\otimes} \psi_n(y). \tag{21}$$

Results

$$\mathcal{T}_{mn}^{(0)} = 9\,; \tag{22}$$

$$\mathcal{T}_{00}^{(1)} = \frac{1}{4}(81 L_\mu + 237)\,; \tag{23}$$

$$\mathcal{T}_{00}^{(2)} = \frac{729 L_\mu^2}{8} - (8\zeta_3 + \frac{35\pi^2}{6} - \frac{4365}{8}) L_\mu + 205\zeta_5 - \frac{3\pi^4}{20} - \frac{759\zeta_3}{2} - \frac{1829\pi^2}{96} + \frac{36559}{32}\,. \tag{24}$$

Analytic continuation

$$\mu^2 \to \mu^2 e^{i\pi}\,. \tag{25}$$

(m,n)	c_1	c_2	d_1	d_2	d_3
(0,0)	20.25	59.25	91.1250	478.436	696.210
(0,2)	32.75	112.473	170.118	1094.39	2025.84
(0,4)	38.45	147.638	211.902	1541.23	3206.98
(0,6)	42.2571	174.359	241.822	1901.22	4265.06
(2,2)	45.25	192.871	266.472	2178.25	4953.36
(2,4)	50.95	240.181	316.173	2875.57	7237.52
(2,6)	54.7571	274.974	351.380	3415.43	9172.70
(4,4)	56.65	292.970	369.484	3704.29	10222.5
(4,6)	60.4571	331.411	407.102	4337.65	12698.8
(6,6)	64.2643	372.282	446.331	5037.27	15588.4

Table: The numerical values for $\mathcal{T}_{mn}^{(1)} = c_1 L_\mu + c_2$ and $\mathcal{T}_{mn}^{(2)} = d_1 L_\mu^2 + d_2 L_\mu + d_3$, with $0 \leq m, n \leq 6$.

Phenomenology

Phenomenology

Input parameters

- QCD light-cone sum rule Ball et al. (2006)JHEP, Mikhailov et al. (2016) PRD, Stefanis (2020) PRD
- Dispersion relation Cheng et al. (2020) PRD See Cheng's talk
- Platykurtic distribution Stefanis (2014) PLB
- Dyson-Schwinger equation Chang et al. (2013) PRL, Raya et al. (2016) PRD
- light-front quark model Choi and Ji 2015 (PRD)
- holographic QCD Chang et al. (2017) PRD
- Lattice QCD Bali et al. (2019) JHEP, Hua et al. (2022) PRL
  See talks by Zhang and Zeng

RQCD: $a_2(2\ \mathrm{GeV}) = 0.116^{+0.019}_{-0.020}$

LPC: $a_2(2\ \mathrm{GeV}) = 0.258 \pm 0.087,\ a_4(2\ \mathrm{GeV}) = 0.122 \pm 0.056,$
$a_6(2\ \mathrm{GeV}) = 0.068 \pm 0.038$

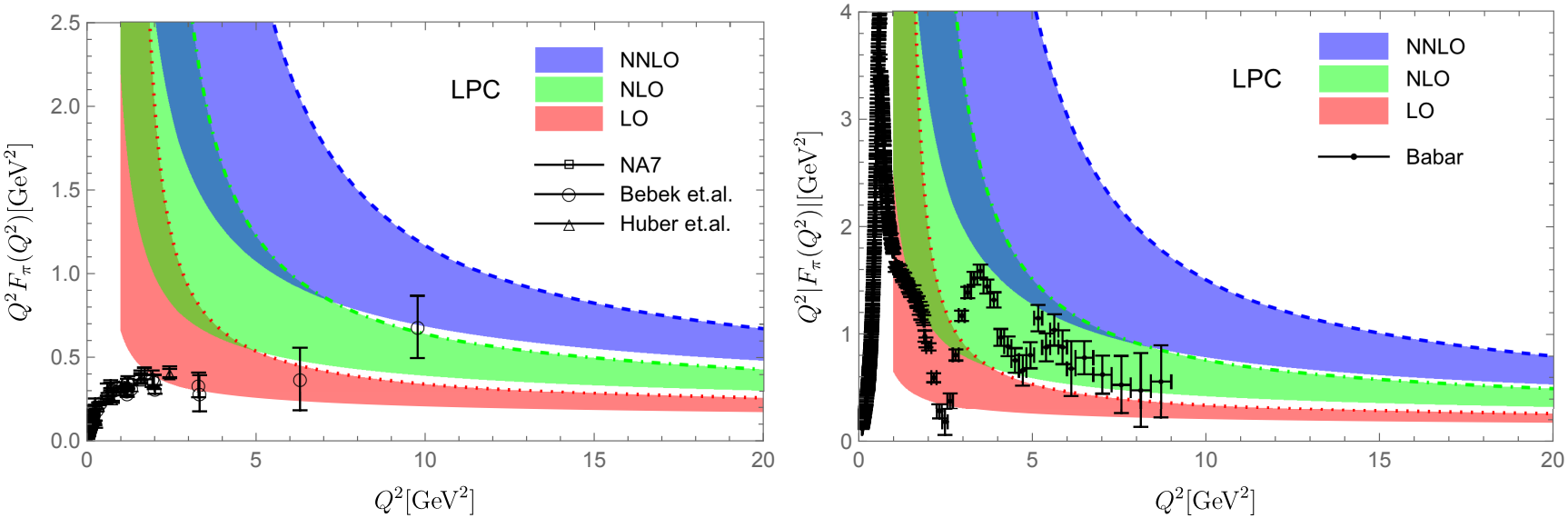

Figure: Theoretical predictions vs. data for $Q^2 F_\pi(Q^2)$ in the space-like (left panel) and time-like (right panel) regions. We take the central values of a_2, a_4 and a_6 determined by `LPC`. The red, green and blue curves correspond to the LO, NLO and NNLO results, and the respective bands are obtained by sliding μ from $Q/2$ to Q. Experimental data points are taken from `NA7`, `Bebek et al.`, `Huber et al.` and `BaBar`.

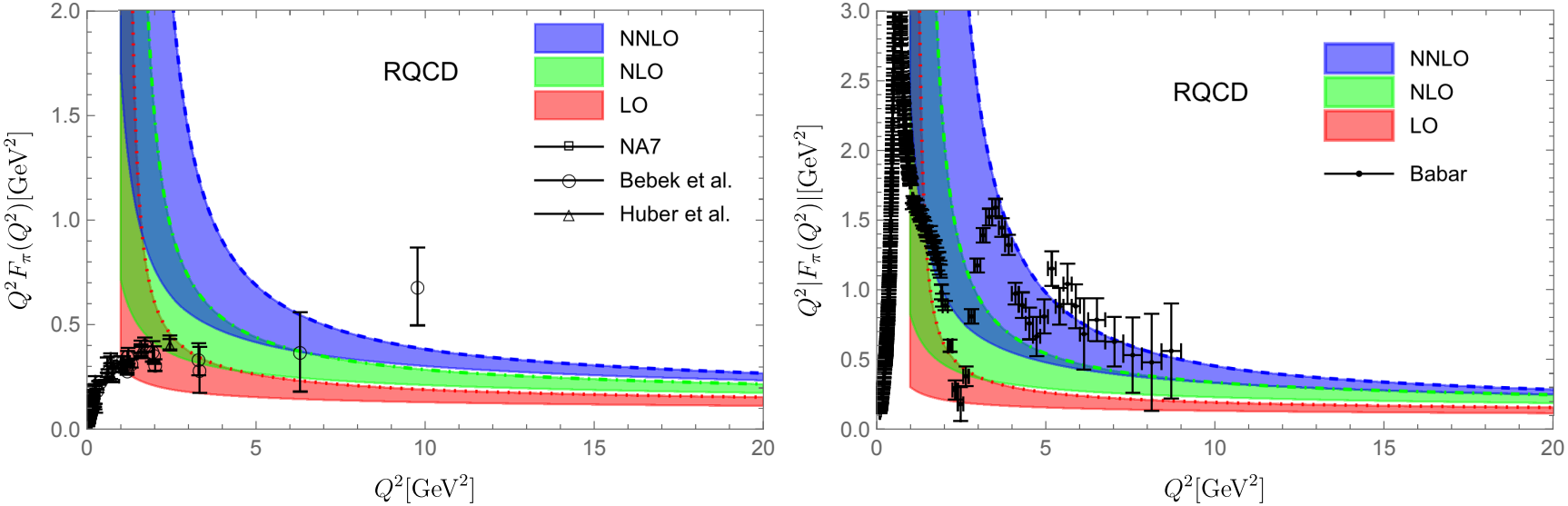

Figure: Same as Fig. 3, except the predictions are made by taking the central value of a_2 determined by RQCD, with a_4 and a_6 set to zero.

Summary

Summary

We calculate the next-to-next-to-leading order (NNLO) QCD radiative correction to the pion electromagnetic form factor with large momentum transfer. We explicitly verify the validity of the collinear factorization to two-loop order for this observable, and obtain the respective IR-finite two-loop hard-scattering kernel in the closed form. The NNLO QCD correction turns to be positive and significant. Incorporating this new ingredient of correction, we then make a comprehensive comparison between the finest theoretical predictions and numerous data for both space-like and time-like pion form factors. Our phenomenological analysis provides strong constraint on the second Gegenbauer moment of the pion light-cone distribution amplitude (LCDA) obtained from recent lattice QCD studies.

Thanks!